AIP | Applied Physics Letters

Hysteretic response of chemical vapor deposition graphene field effect transistors on SiC substrates

Edward Cazalas, Isaac Childres, Amanda Majcher, Ting-Fung Chung, Yong P. Chen et al.

Citation: Appl. Phys. Lett. **103**, 053123 (2013); doi: 10.1063/1.4816426
View online: http://dx.doi.org/10.1063/1.4816426
View Table of Contents: http://apl.aip.org/resource/1/APPLAB/v103/i5
Published by the AIP Publishing LLC.

Hysteretic response of chemical vapor deposition graphene field effect transistors on SiC substrates

Edward Cazalas,[1,a)] Isaac Childres,[2,3] Amanda Majcher,[1] Ting-Fung Chung,[2,3] Yong P. Chen,[2,3,4] and Igor Jovanovic[1]
[1]*Department of Mechanical and Nuclear Engineering, The Pennsylvania State University, University Park, Pennsylvania 16802, USA*
[2]*Department of Physics, Purdue University, West Lafayette, Indiana 47907, USA*
[3]*Birck Nanotechnology Center, Purdue University, West Lafayette, Indiana 47907, USA*
[4]*School of Electrical and Computer Engineering, Purdue University, West Lafayette, Indiana 47907, USA*

(Received 23 April 2013; accepted 30 June 2013; published online 2 August 2013)

Graphene field effect transistors (GFETs) fabricated by chemical vapor deposition graphene deposited onto SiC substrates exhibit sensitivity to broadband visible light. The hysteretic nature of this GFET type was studied utilizing a new current-voltage measurement technique in conjunction with current-time measurements. This measurement method accounts for hysteretic changes in graphene response and enables transfer measurements that can be attributed to fixed gate voltages. Graphene hysteresis is shown to be consistent with electrochemical p-type doping, and current-time measurements clearly resolve a hole to electron to hole carrier transition in graphene with a single large change in gate voltage. © *2013 AIP Publishing LLC*. [http://dx.doi.org/10.1063/1.4816426]

The unique properties of single layer graphene, such as its high electrical conductivity, large carrier mobility, and ambipolar behavior make it an attractive material of study for electrical device applications.[1–3] The ambipolarity of response of graphene is manifested by a maximum in resistivity at a given external electric field, known as the Dirac point.[4] Near the Dirac point, the resistance of graphene is especially sensitive to local changes in electric field, enabling the development of graphene field effect transistors (GFETs) with unique operational characteristics that result from this ambipolar response.[5,6]

Hysteretic effects have been widely observed in current-voltage (I_{sd}-V_{bg}, sd = source–drain, bg = backgate) transfer measurements of GFETs, causing the shape of the transfer curve and the location of the Dirac point to be dependent on direction, speed, and range with which gate voltage sweeps are performed.[7–11] The origin of this hysteresis has been shown to be electrochemical doping of the substrate material on which graphene is deposited.[12] Electrochemical p-type doping may be introduced during device fabrication, or after exposure to environments containing H_2O and O_2, or NO_2.[13–15] Electrochemical doping involves electron transfer to or from graphene via a redox reaction: $O_2 + 2H_2O + 4\,e^-$ (graphene) $\rightleftarrows 4OH^-$. The direction of the reaction is determined by the relative height of Fermi energy levels of the graphene and the redox solution, the former being controlled by gate bias and the latter by the density of redox states.[13,15]

Systematic studies have explored the hysteresis occurring in GFETs on Si/SiO_2 substrates[7–11,15,16] by varying the I_{sd}-V_{bg} sweep parameters. The time evolution of graphene resistance in the presence of electrochemical species on Si/SiO_2[13,14,17–19] and in aqueous solution[20] has also been studied. While previous studies have already examined the hysteresis effect of chemical vapor deposition (CVD) graphene on Si/SiO_2,[21–23] this letter provides insight into the hysteretic nature of GFETs utilizing CVD graphene on SiC substrates. This insight arises from the use of a time-dependent characterization of the GFET through graphene current vs. time (I_{sd}-t) measurements. To aid in I_{sd}-t measurement analysis, an I_{sd}-V_{bg} technique was developed that measures a graphene transfer curve while being effectively kept at a fixed gate voltage. In all measurements, current (I_{sd}) is converted to resistance. Such studies can provide understanding into the operation of graphene-based devices with hysteretic behavior for memory devices,[21,24–27] chemical sensing,[14,18,20,28–31] photodetectors,[32,33] and ionizing radiation detectors.[34]

Since SiC is a semiconductor with a bandgap of approximately 3 eV (at 300 K for 6 H), its conductivity is sensitive to photons with $\lambda \lesssim 413$ nm. Photons of these wavelengths are available on the UV end of the broadband visible light spectrum. In the absence of illumination by broadband visible light, the SiC substrate is highly resistive, and the applied backgate voltage, V_{bg}, drops uniformly across the substrate. The relatively large thickness of the SiC substrate (in our design $d_{SiC} = 300\,\mu$m) results in a relatively small electric field ($E = V_{bg}/d_{SiC}$ in a plate capacitor model). Graphene resistance is then governed primarily by the electric field resulting from trapped charges. When exposed to broadband visible light, the SiC substrate becomes partially conductive, increasing the electric field present at the graphene. Experiments show that the exposure to light can induce a sufficiently large change of electric field to overcome the capacitive shielding produced by trapped charges, as evidenced by the presence of Dirac peaks in Figure 1. To effectively characterize the GFET resistance in the vicinity of Dirac point by use of moderate backgate voltages, the top of the GFET was exposed to broadband visible light. The light was provided by a 13 W compact fluorescent bulb. The entire SiC chip area (0.3 cm^2) was exposed to the light. The Dirac point voltage, V_d, is dependent on the voltage sweep direction, as evident in Figure 1 and reported in prior studies.[7,8,11] The positive values of V_d indicate p-type doping of

a)Electronic mail: ejc149@psu.edu

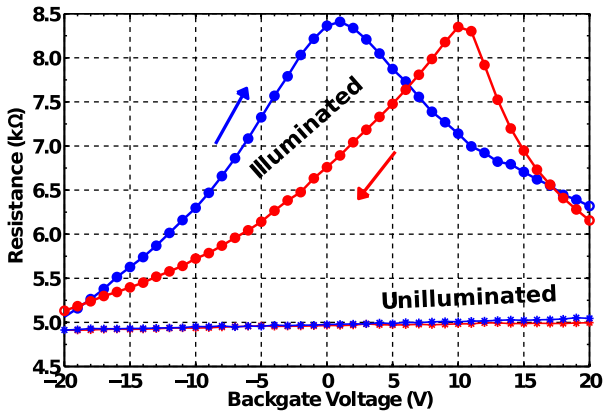

FIG. 1. Transfer curves (I_{sd}-V_{bg}) with GFET in illuminated and unilluminated conditions. The sweeps are performed with backgate voltage changing in "forward" (red) and "backward" (blue) directions, indicated by the arrows. A sweep speed of $|dV_{bg}| = 1$ V/s was utilized. Hysteresis of Dirac points of 9 V was observed when GFET is illuminated. The conductance at V_d was 29.7 μS/square (graphene dimensions are 4×1 μm).

graphene, and the hysteretic and doping characteristics in Figure 1 are consistent with electrochemical doping.[15,24] Graphene measurements were conducted at room temperature and in ambient air.

Many studies have been conducted to characterize the dependence of the GFET hysteresis on sweep speed (V/s).[7–9,21,23–25] Figure 2 illustrates the underlying cause of this dependence in our experiment. Graphene resistance varies significantly with time when responding to changes of backgate voltage. High rates of voltage change were utilized to obtain a better insight into the hysteretic behavior. As observed in Figure 2, graphene resistance eventually stabilizes, reaching an asymptotic value. Stabilization (or relaxation) requires applying a single backgate voltage on the order of the period required for the density of redox states to come to equilibrium in response to a change in electric field by a gate voltage.[12] The time for graphene resistance to fully stabilize in response to a change in backgate voltage is on the order of minutes, and is comparable to that observed in previous studies.[21,24]

A measurement technique was developed which is particularly suitable to simultaneously (1) minimize the hysteresis induced by the measurement and (2) obtain the transfer curves for a hysteretic GFET at any given operating voltage. The technique is based on an I_{sd}-V_{bg} measurement method that stabilizes the graphene resistance at a backgate voltage between discrete voltage sweep steps. While this I_{sd}-V_{bg} measurement method is similar to "pulse" type transfer measurements,[8,35–38] this technique was developed to allow transfer curve characterization at any given V_{bg} that may be desired for GFET operation while also considering the graphene response speed. It was empirically determined that the amount of time usually required to reach a resistance minimum immediately following a step change in sweep voltage was ~10 s, as shown in Figure 2. The resistance minimum during application of sweep voltage is selected as a point of importance as it is when hysteretic effects begin to dominate graphene response. A 20 s stabilization time was selected, sufficiently long for graphene resistance to stabilize, except when there was a significant difference between the sweep voltage and the selected stabilization voltage. This is illustrated in I_{sd}-t response in Figure 3, which shows that as sweep voltages become greater than $V_{bg} = 9$ V (or at times greater than 890 s), the graphene resistance no longer stabilizes over the same period. However, this incomplete stabilization does not affect V_d. The switching of the backgate voltage between sweep and stabilization voltages causes the oscillating behavior in graphene resistance in Figure 3. Figure 3 illustrates how an I_{sd}-V_{bg} transfer curve is generated from an I_{sd}-t measurement. The I_{sd}-t measurement is conducted by switching the backgate voltage between the stabilization voltage ($V_{bg} = -20$ V) and a monotonically increasing sweep voltage, which steps from $V_{bg} = -20$ V to +20 V in 1 V intervals. The resistance of graphene at the end of each sweep interval in the I_{sd}-t measurement is recorded as the resistance for that backgate voltage in the I_{sd}-V_{bg} transfer curve. As shown in Figure 3, the resistances recorded from the I_{sd}-t measurement are traced, forming the transfer curve shown in Figure 4 (for a forward sweep at $V_{bg} = -20$ V).

Using the described I_{sd}-V_{bg} measurement method, the transfer curves for backgate stabilization voltages of $V_{bg} = -20$, 0, and +20 V were measured and are shown in

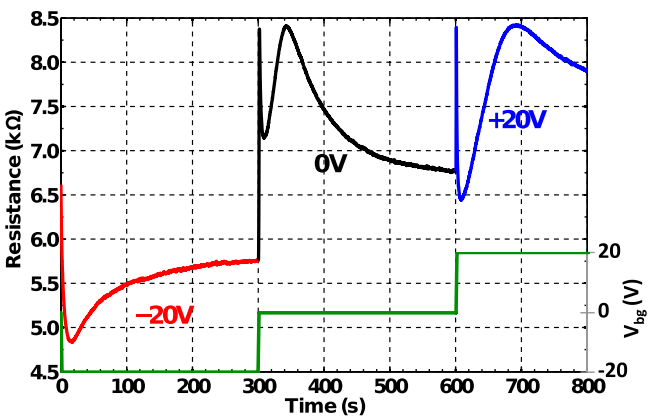

FIG. 2. Time dependent hysteretic graphene response (I_{sd}-t) from instantaneous change in backgate voltage for $V_{bg} = -20$ V (0–300 s, red) to 0 V (300–600 s, black) to +20 V (600–800 s, blue). The applied backgate voltage (V_{bg}) time profile is shown in green (right axis). $V_{bg} = 0$ V at the beginning of the measurement.

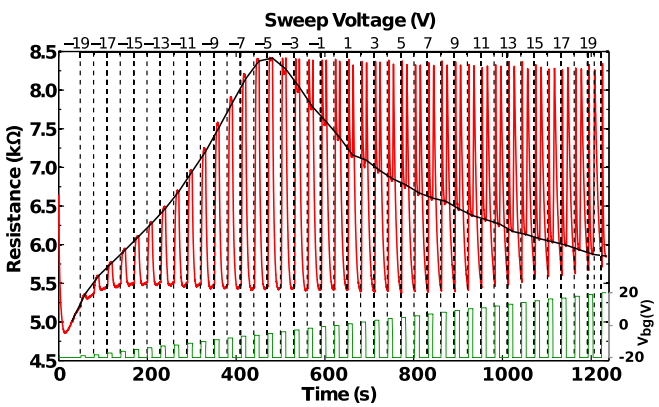

FIG. 3. Time dependent graphene resistance (red, left axis) in I_{sd}-t forward-sweep measurement for a stabilization voltage of $V_{bg} = -20$. The time dependence of V_{bg} is shown in green (right axis). Each grid spacing comprises 30 s; the first 10 s was used to apply the sweep voltage, while the last 20 s was used to allow stabilization at $V_{bg} = -20$ V. A guide to eye transfer curve (black) was traced through recorded data points taken for I_{sd}-V_{bg} measurements, matching the Dirac peak given in Figure 4 for a forward sweep with stabilization $V_{bg} = -20$ V. At time 0 s, backgate voltage shifts from $V_{bg} = 0$ V to −20 V.

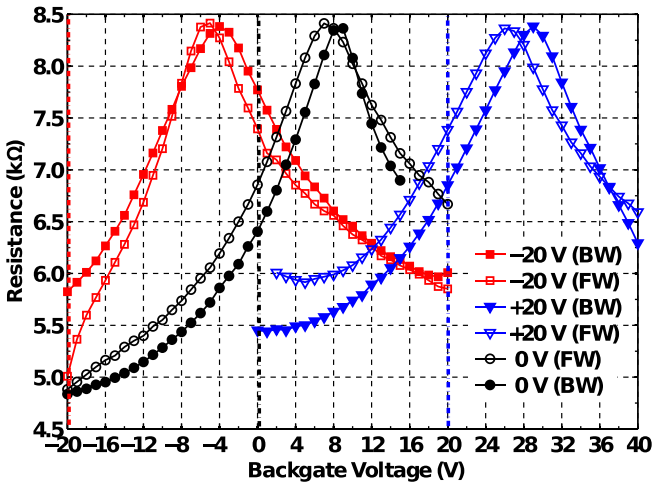

FIG. 4. Transfer curves (I_{sd}-V_{bg}) with stabilization at $V_{bg} = -20$ V (red), 0 V (black), and +20 V (blue) for forward (FW) and backward (BW) sweep directions. The vertical dotted lines represent voltage of stabilization/operation respective to the same color transfer curve. The Dirac peaks are located above the respective stabilization voltages. The unfilled and filled data points represent forward and backward sweeps, respectively. Hysteresis of the Dirac point is reduced to 1, 2, and 3 V for $V_{bg} = -20$ V, 0 V, and +20 V, respectively.

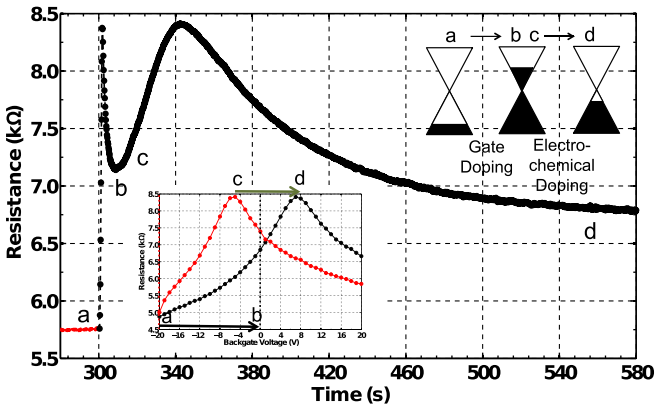

FIG. 5. An expanded view of Figure 2 (280–580 s), showing the I_{sd}-t response with backgate change of $V_{bg} = -20$ V (red) to 0 V (black). The bottom inset shows the experimentally obtained transfer curves using the developed I_{sd}-V_{bg} method for backgate voltages stabilized at $V_{bg} = -20$ V (red) and 0 V (black). The upper inset shows the energy spectrum of graphene carriers. Both inset figures illustrate the abrupt increase of the graphene Fermi energy in response to a backgate change (a to b) and the Dirac peak shifting due to charge transfer from graphene to doping species (c to d).

Figure 4. The measured V_d hysteresis was considerably reduced for all stabilization voltages by use of this measurement method, as can be seen by comparing Figures 1 and 4. Transfer curves exhibit the characteristics consistent with electrochemical p-type doping of graphene, as V_d shifts in the direction opposite to the sweep direction.[15,24] The residual hysteresis present when this measurement method was applied is due to the selected voltage stabilization step period not being long enough for a complete stabilization of graphene resistance to occur. The developed I_{sd}-V_{bg} measurement technique can be used to appropriately account for the hysteretic response of graphene when used as a sensor, where a time-dependent resistance measured within a period of time constitutes the signal. This signal can be correlated to the transfer curve generated by the described method so long as the transfer curve had been measured with the voltage sweep step time comparable to the characteristic duration of the signal.

The features of graphene response in Figure 2 can now be explained with the aid of the I_{sd}-V_{bg} measurement method. An expanded view of I_{sd}-t response with backgate voltage shift of $V_{bg} = -20$ V to 0 V is provided as an example in Figure 5. The lower inset displays transfer curves stabilized at $V_{bg} = -20$ V and 0 V (forward sweeps). Two key features are present in I_{sd}-t response to a change in backgate voltage observed in our GFET. The first feature (a, b) is dominated by the capacitance formed by the backgate and graphene. The slow response speed of our GFET (backgate leakage time constant $\approx$ 0.33 s) allowed the Dirac point to be distinctly observed between time points "a" and "b," following a change in backgate voltage. As the V_d point is crossed, the graphene switches from hole to electron carrier type. In related experiments we conducted, the transient occurrence of the Dirac point could not be observed in exfoliated graphene on doped Si due to the relatively small capacitance that results in fast device response, similar to observations by Martínez *et al.*[20] and Wu *et al.*[28] As evidenced in Figure 5, the inflection point "b" has a minimum resistance that is approximately equal to the resistance at $V_{bg} = 0$ V in the transfer curve stabilized at $V_{bg} = -20$ V. The second feature, occurring between points "c" and "d" in Figure 5, arises from the trapping of electrons from graphene by the underlying dopant species through redox reactions, causing the eventual p-doping of graphene. During this time, V_d slowly shifts from −5 V to 7 V and the graphene reverts back to hole from electron carrier type. Graphene resistance in Figure 5 eventually approaches the resistance at $V_{bg} = 0$ V for a transfer curve stabilized at $V_{bg} = 0$ V in Figure 4. In retrospect, each voltage sweep step of Figure 3 can be explained similarly for $V_{bg} > V_d$. When $V_{bg} < V_d$, the Dirac point is not crossed and therefore not observed in I_{sd}-t measurements. It is expected that performing the I_{sd}-t measurement, as done in Figures 2 and 5, in the backward direction ($V_{bg} = +20$ V to 0 V to −20 V) will maintain hole carrier type in graphene, as the Dirac point is never traversed.

The hysteretic nature of CVD graphene on SiC substrates was experimentally studied and found to be consistent with electrochemical doping through redox reactions. Our GFET[39] was also found to be sensitive to broadband visible light. The hysteretic behavior was studied with complimentary I_{sd}-V_{bg} and I_{sd}-t measurements, which reveal a response consisting of a fast and a slow component. The fast component is attributed to GFET capacitance, while the slow component is attributed to electron transfer through redox reaction. Graphene carrier type was observed to switch from hole to electron, and back to hole following a relatively large positive change in backgate voltage. To aid the understanding and analysis of the hysteretic I_{sd}-t response, an I_{sd}-V_{bg} measurement technique was developed that accounts for the graphene hysteresis. This technique enables the characterization of hysteretic GFET response while at a desired operating gate voltage, useful in signal detection applications that rely on modifying the local electric field experienced by graphene.

This work was funded in part by the Department of Homeland Security (DHS) and the National Science Foundation (NSF) through the Academic Research Initiative

(ARI) (2009-DN-077-ARI036-02) and by the Defense Threat Reduction Agency (DTRA).

[1]K. S. Novoselov, A. K. Geim, S. V Morozov, D. Jiang, M. I. Katsnelson, I. V Grigorieva, S. V Dubonos, and A. A. Firsov, Nature **438**, 197 (2005).
[2]T. J. Echtermeyer, M. C. Lemme, J. Bolten, M. Baus, M. Ramsteiner, and H. Kurz, Eur. Phys. J. Spec. Top. **148**, 19 (2007).
[3]S. V. Morozov, K. S. Novoselov, M. I. Katsnelson, F. Schedin, D. C. Elias, J. A. Jaszczak, and A. K. Geim, Phys. Rev. Lett. **100**, 016602 (2008).
[4]A. N. Grigorenko, M. Polini, and K. S. Novoselov, Nat. Photonics **6**, 749 (2012).
[5]Z. Chen and J. Appenzeller, in *Electron Devices Meeting, IEDM 2008, San Fransisco, USA, Dec. 15–17 2008* (IEEE International, 2008), pp. 1–4.
[6]F. Schwierz, Nat. Nanotechnol. **5**, 487 (2010).
[7]G. Kalon, Y. J. Shin, V. G. Truong, A. Kalitsov, and H. Yang, Appl. Phys. Lett. **99**, 083109 (2011).
[8]Z.-M. Liao, B.-H. Han, Y.-B. Zhou, and D.-P. Yu, J. Chem. Phys. **133**, 044703 (2010).
[9]P. Joshi, H. E. Romero, A. T. Neal, V. K. Toutam, and S. A. Tadigadapa, J. Phys. Condens. Matter **22**, 334214 (2010).
[10]J. Chen, J. Li, J. Yang, X. Yan, B. K. Tay, and Q. Xue, Appl. Phys. Lett. **99**, 173104 (2011).
[11]P. J. Wessely, F. Wessely, E. Birinci, B. Riedinger, and U. Schwalke, Electrochem. Solid-State Lett. **15**, K31 (2012).
[12]H. Pinto, R. Jones, J. P. Goss, and P. R. Briddon, Phys. Status Solidi A **207**, 2131 (2010).
[13]P. L. Levesque, S. S. Sabri, C. M. Aguirre, J. Guillemette, M. Siaj, P. Desjardins, T. Szkopek, and R. Martel, Nano Lett. **11**, 132 (2011).
[14]F. Schedin, a. K. Geim, S. V. Morozov, E. W. Hill, P. Blake, M. I. Katsnelson, and K. S. Novoselov, Nature Mater. **6**, 652 (2007).
[15]H. Xu, Y. Chen, J. Zhang, and H. Zhang, Small **8**, 2833 (2012).
[16]S. Unarunotai, Y. Murata, C. E. Chialvo, H. Kim, S. MacLaren, N. Mason, I. Petrov, and J. A. Rogers, Appl. Phys. Lett. **95**, 202101 (2009).
[17]A. A. Kaverzin, S. M. Strawbridge, A. S. Price, F. Withers, A. K. Savchenko, and D. W. Horsell, Carbon **49**, 3829 (2011).
[18]R. S. Sundaram, C. Gómez-Navarro, K. Balasubramanian, M. Burghard, and K. Kern, Adv. Mater. **20**, 3050 (2008).
[19]Z. Liu, A. A. Bol, and W. Haensch, Nano Lett. **11**, 523 (2011).
[20]J. G. Martínez, T. F. Otero, C. Bosch-Navarro, E. Coronado, C. Martí-Gastaldo, and H. Prima-Garcia, Electrochim. Acta **81**, 49 (2012).
[21]G. R. Turpu, M. W. Iqbal, M. Z. Iqbal, and J. Eom, Thin Solid Films **522**, 468 (2012).
[22]J. Chan, A. Venugopal, A. Pirkle, S. McDonnell, D. Hinojos, C. W. Magnuson, R. S. Ruoff, L. Colombo, R. M. Wallace, and E. M. Vogel, ACS Nano **6**, 3224 (2012).
[23]W. Li, C. Tan, M. Lowe, H. Abruña, and D. Ralph, ACS Nano **5**, 2264 (2011).
[24]H. Wang, Y. Wu, C. Cong, J. Shang, and T. Yu, ACS Nano **4**, 7221 (2010).
[25]E. B. Song, B. Lian, S. Min Kim, S. Lee, T.-K. Chung, M. Wang, C. Zeng, G. Xu, K. Wong, Y. Zhou, H. I. Rasool, D. H. Seo, H.-J. Chung, J. Heo, S. Seo, and K. L. Wang, Appl. Phys. Lett. **99**, 042109 (2011).
[26]S. A. Imam, T. Deshpande, A. Guermoune, M. Siaj, and T. Szkopek, Appl. Phys. Lett. **99**, 082109 (2011).
[27]S. Lee, E. B. Song, S. Kim, D. H. Seo, S. Seo, T. Won Kang, and K. L. Wang, Appl. Phys. Lett. **100**, 023109 (2012).
[28]W. Wu, Z. Liu, L. A. Jauregui, Q. Yu, R. Pillai, H. Cao, J. Bao, Y. P. Chen, and S.-S. Pei, Sens. Actuators B **150**, 296 (2010).
[29]Y. Lu, B. R. Goldsmith, N. J. Kybert, and a. T. C. Johnson, Appl. Phys. Lett. **97**, 083107 (2010).
[30]Y. Ohno, K. Maehashi, and K. Matsumoto, Biosens. Bioelectron. **26**, 1727 (2010).
[31]D. Chen, L. Tang, and J. Li, Chem. Soc. Rev. **39**, 3157 (2010).
[32]N. Kurra, V. S. Bhadram, C. Narayana, and G. U. Kulkarni, Nanotechnology **23**, 425301 (2012).
[33]Z. Sun, Z. Liu, J. Li, G.-A. Tai, S.-P. Lau, and F. Yan, Adv. Mater. **24**, 5878 (2012).
[34]O. Koybasi, I. Childres, I. Jovanovic, and Y. P. Chen, Proc. SPIE **8373**, 83730H (2012).
[35]M. H. Ervin, A. M. Dorsey, and N. M. Salaets, Nanotechnology **20**, 345503 (2009).
[36]Y. G. Lee, C. G. Kang, U. J. Jung, J. J. Kim, H. J. Hwang, H.-J. Chung, S. Seo, R. Choi, and B. H. Lee, Appl. Phys. Lett. **98**, 183508 (2011).
[37]D. Estrada, S. Dutta, A. Liao, and E. Pop, Nanotechnology **21**, 85702 (2010).
[38]E. Carrion, A. Malik, A. Behnam, S. Islam, and E. Pop, in *Proceedings of the 70th Device Research Conference, University Park, USA, June 18-20 2012* (IEEE, 2012), pp. 183–184.
[39]See supplementary material at http://dx.doi.org/10.1063/1.4816426 for description of device fabrication process, GFET design parameters, and testing equipment.